Nanoscale Hybrid Electrolytes with Viscosity Controlled Using Ionic Stimulus for Electrochemical Energy Conversion and Storage

Sara T. Hamilton, Tony G. Feric, Sahana Bhattacharyya, Nelly M. Cantillo, Steven G. Greenbaum, Thomas A. Zawodzinski, and Ah-Hyung Alissa Park*

Cite This: *JACS Au* 2022, 2, 590−600 | Read Online

ACCESS | Metrics & More | Article Recommendations | SI Supporting Information

ABSTRACT: As renewable energy is rapidly integrated into the grid, the challenge has become storing intermittent renewable electricity. Technologies including flow batteries and CO_2 conversion to dense energy carriers are promising storage options for renewable electricity. To achieve this technological advancement, the development of next generation electrolyte materials that can increase the energy density of flow batteries and combine CO_2 capture and conversion is desired. Liquid-like nanoparticle organic hybrid materials (NOHMs) composed of an inorganic core with a tethered polymeric canopy (e.g., polyetheramine (HPE)) have a capability to bind chemical species of interest including CO_2 and redox-active species. In this study, the unique response of NOHM-I-HPE-based electrolytes to salt addition was investigated, including the effects on solution viscosity and structural configurations of the polymeric canopy, impacting transport behaviors. The addition of 0.1 M NaCl drastically lowered the viscosity of NOHM-based electrolytes by up to 90%, reduced the hydrodynamic diameter of NOHM-I-HPE, and increased its self-diffusion coefficient, while the ionic strength did not alter the behaviors of untethered HPE. This study is the first to fundamentally discern the changes in polymer configurations of NOHMs induced by salt addition and provides a comprehensive understanding of the effect of ionic stimulus on their bulk transport properties and local dynamics. These insights could be ultimately employed to tailor transport properties for a range of electrochemical applications.
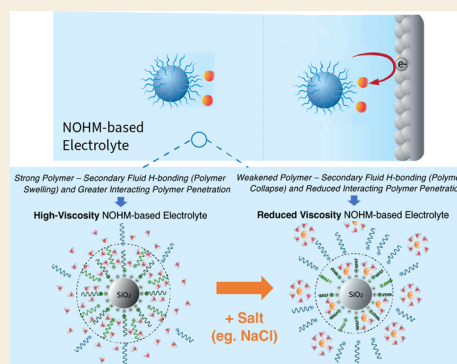
KEYWORDS: nanoparticle organic hybrid materials, electrolyte, viscosity, diffusion, flow battery, CO_2 capture and conversion

INTRODUCTION

Due to the intermittent nature of renewable energy, there is a growing need to develop versatile options for large-scale energy storage.[1,2] Both batteries and electrochemical conversion of CO_2 to dense energy carriers have emerged as means of storing carbon-free renewable energy. The design and selection of electrolytes are key components of these emerging electrochemical energy storage systems, mediating ion transport behaviors and enhanced solubility to ultimately deliver high energy and power density systems.[3−5] A number of novel electrolyte chemistries have been studied for electrochemical energy storage applications, including ionic liquids (ILs),[6−10] deep eutectic solvents (DES),[6,11−14] and redox-active polymers (RAPs).[15−20]

ILs and DES have recently attracted attention in the field of energy storage because of their suitable electrolyte properties, including high thermal stability, low-to-negligible volatility, wide voltage windows, nonflammability, and low toxicity.[11] Furthermore, ILs and DES offer opportunities to increase the solubility of redox-active species in solution (and thereby, the energy density of electrochemical systems) due to their high solvation strength of various reactive species.[9,21−23] The main challenge associated with the incorporation of ILs and DES in energy storage systems is their inherently low ionic conductivity (typically <10 mS/cm at 25 °C) associated with high solution viscosity, which limits power density achievable in redox-flow batteries.[24−28] Thus, the development of strategies to lower the viscosity of ILs and DES has been an area of ongoing research.[27−32] RAPs are another class of novel electrolytes offering opportunities for energy storage systems due to their ability to be coupled with an inexpensive size-exclusion membrane because of their macromolecular nature. In the same way as ILs and DES, RAPs are challenged by their high viscosity, in addition to other challenges including their low solubility and sensitivity to electrochemical degradation.

Liquid-like nanoparticle organic hybrid materials (NOHMs) are a class of hybrid materials that have recently been explored as components of novel electrolytes. They consist of an inorganic core to which polymeric chains ("canopy") are
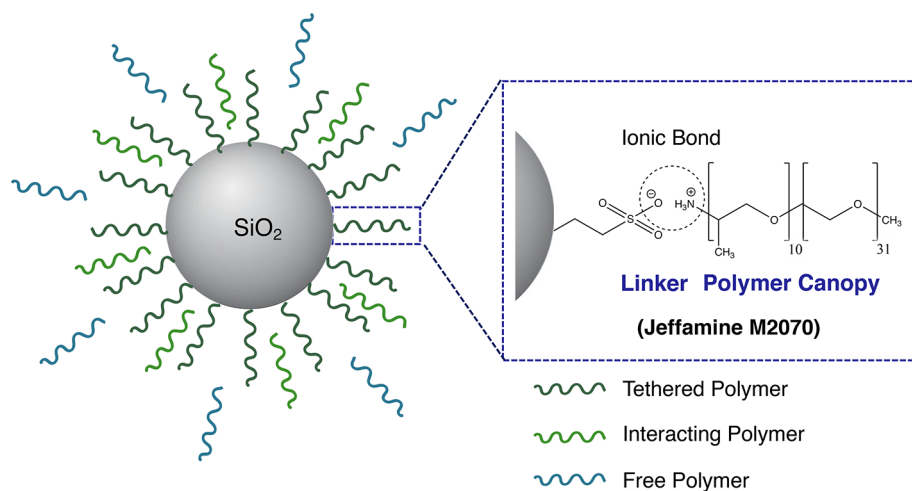
Figure 1. Structure of liquid-like nanoparticle organic hybrid materials (NOHM-I-HPE, where HPE = Jeffamine M2070), including tethered, interacting, and free polymer.

tethered ionically, as shown in Figure 1.[33] Haque et al. recently reported on the use of small-angle neutron scattering (SANS) to probe the dispersion and structure of ionic NOHM-I-HPE in aqueous solution. The study found that there exists a distribution of polymer states in these systems including tethered polymer, free polymer, and interacting polymer.[62] These three distinct classes of polymers are illustrated in Figure 1 and are defined as follows: (i) tethered polymer, a polymer that is grafted (ionically bonded) to the functionalized SiO_2 nanoparticles; (ii) interacting polymer, free polymer that penetrates the grafted layer; and (iii) free polymer, polymer chains that exist in the bulk solution.

NOHMs boast a high degree of chemical and physical tunability, with a wide range of nanocore−canopy combinations possible for a variety of functionalities. They exhibit negligible vapor pressure and a higher thermal and oxidative stability compared to those of their constituent polymers.[33−35] NOHMs were initially developed by Archer et al. as electrolyte additives to suppress dendritic growth in battery applications[36−40] and were explored by Park et al. as anhydrous CO_2 capture solvents.[33−35,41−43] The synthesis, dynamics, and CO_2 capture mechanisms of various classes of NOHMs have been extensively investigated.[33−35,41−44] NOHMs interact with other chemical species based both on enthalpic and entropic contributions, which are influenced by the functional groups along the polymer chains and the structural configurations of the NOHMs' polymeric canopy, respectively.[43] Recently, NOHM-based fluids have been explored as potential novel electrolytes in electrochemical applications[45] and for combined CO_2 capture and conversion[46,47] based on their ability to complex redox-active species and selectively capture CO_2.

Similar to other novel fluids including ILs, the current challenge of NOHMs in these energy and environmental applications[33−35,41−43,48−51] is their inherently high viscosity, as the viscosity of the neat NOHMs approaches 15,000 cP.[34] To overcome the high viscosity of NOHMs for CO_2 capture applications, microencapsulation and solvent-impregnated polymers (SIPs) using a UV-curable polymeric shell with high CO_2 permeability has been investigated.[48−51] These encapsulation techniques are very effective at accelerating CO_2 capture kinetics of NOHMs designed for carbon capture, but NOHMs are now employed as a micron-sized, packaged particulate system rather than a solvent system.

The viscosity and ionic conductivity of the electrolyte are key factors in electrochemical energy storage applications, as they limit achievable charge transport and reaction kinetics, strongly impacting electrochemical performance.[52] High viscosities and low ionic conductivities continue to challenge the use of novel electrolyte chemistries, such as ILs[24,25] and DES.[26−28] Thus, innovative approaches are required to tune the viscosity and conductivity of NOHM-based electrolytes. Viscosity control is also critical for pumping fluids in and out of a reactor system, as viscosities above 40−60 cP are generally considered to be highly energy intensive.[46]

Recently, we found that the addition of salt (e.g., NaCl) can significantly reduce the viscosity of NOHM-based electrolytes.[62] Giannelis and co-workers also investigated the introduction of electrolyte ions on the local and collective dynamics of neat NOHMs and found that their addition results in faster canopy exchange and lowered bulk viscosity.[53] However, a fundamental understanding of the mechanisms and the key parameters of this phenomenon in aqueous solution have not been revealed yet. Thus, this study is designed to determine the effect of ionic stimulus on the chemical and physical properties of the binary mixtures of NOHMs with water. Alterations in the conformational structure of the NOHMs' polymeric canopy with the addition of salt are probed using dynamic light scattering (DLS) to explain the trends in measured bulk physicochemical properties. Additionally, ^1H and ^{23}Na NMR diffusion measurements were performed to characterize the effect of added NaCl on intermolecular interactions between constituent NOHMs' polymer and the secondary fluid (i.e., water) and ionic transport behaviors. This study thus provides a comprehensive understanding of the effect of ionic stimulus on both bulk transport properties and on the local dynamics of NOHM-I-HPE-based electrolytes, by examining changes in the conformation of the polymeric canopy as well as transport of water and salt molecules present in the electrolyte solution.

■ EXPERIMENTAL SECTION

NOHM Synthesis

NOHM-I-HPE was synthesized as detailed in previous work.[33,42,54] "I" is used to indicate that the bond between the linker molecule and the polymeric canopy is ionic, and "HPE" indicates that the constituent polymer is polyetheramine ("PE") with a high ("H")
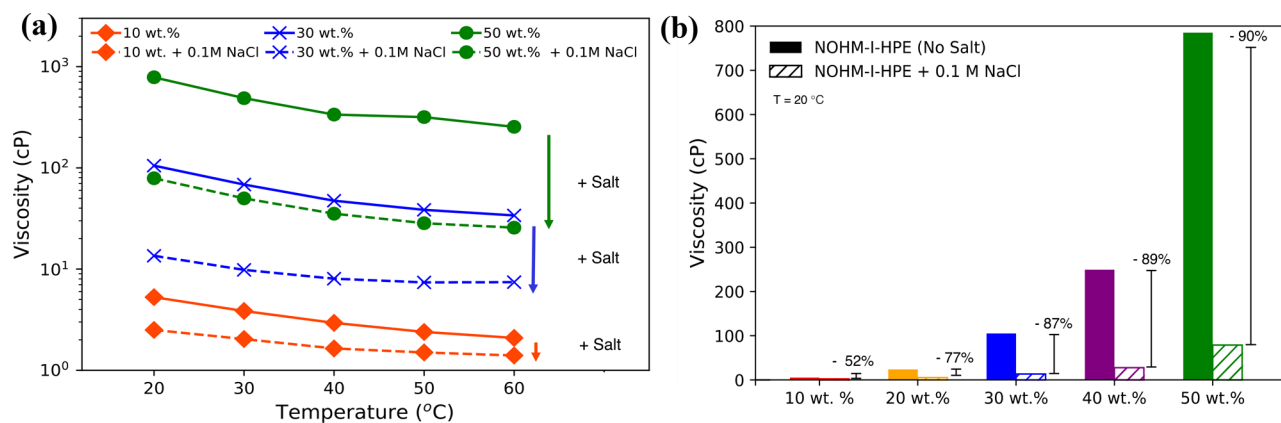
Figure 2. Effect of salt addition on the viscosity of the NOHM-based fluids. (a) Viscosities of NOHM-I-HPE solutions as a function of temperature. Dashed lines represent NOHM-I-HPE solutions with 0.1 M NaCl addition. (b) Percentage decrease in viscosity of NOHM-I-HPE solutions of 10, 20, 30, 40, and 50 wt % NOHM loading with the addition of 0.1 M NaCl at 20 °C.

content of ether groups. In short, 6 wt % 3-(trihydroxysilyl)-1-propanesulfonic acid (Gelest, Inc.) and 3 wt % silica nanoparticles (Ludox HS-30, 7 nm, Sigma-Aldrich) aqueous solutions were prepared, and the silica suspension was added dropwise to the silane mixture. After the mixture pH was adjusted to 5 by 1 M NaOH addition, it was stirred for 24 h at 70 °C to facilitate the grafting reaction between the silica nanoparticle and the linker. Excess linker was removed via 48 h of dialysis (3500 molecular weight cutoff (MWCO), Thermo Scientific) against deionized water. To replace the Na^+ ions on the surface of the functionalized SiO_2 nanoparticles with protons, the linker-grafted solution was passed through a cation exchange resin column (Dowex HCR-W2, Sigma-Aldrich). Then, a 10 wt % Jeffamine M2070 (HPE, MW 2000, Huntsman Co.) solution was prepared and added dropwise to the functionalized nanoparticle suspension until the equivalence point, where all the linker sulfonate groups were neutralized. The final product was oven-dried overnight at 65 °C to remove all water from the prepared NOHM-I-HPE. The resulting structure of NOHM-I-HPE is given in Figure 1.

Preparation of NOHM-Based Fluids with and without Salt Addition

Binary mixtures of the NOHM-I-HPE and deionized water were prepared using an analytical balance (ML104T, Mettler Toledo) with a precision of 10^{-4} g. Prior to sample preparation, the NOHM-I-HPE was dried again under vacuum at 60 °C for 3 h to ensure the removal of any excess moisture. The following NOHM-I-HPE samples were prepared: 10, 20, 30, 40, and 50 wt %. Solutions of NOHM-I-HPE containing salts were prepared by adding 0.025, 0.05, 0.1, 0.5, and 1.0 M NaCl (Sigma-Aldrich, ACS, ≥99.0%). The NaCl concentrations are given in terms of its concentrations in the prepared NOHM-I-HPE fluids. Samples were mixed in 10 mL volumetric flasks until complete dissolution of the salt was observed. Solutions of Jeffamine M2070 (HPE) were also prepared following the same procedure. To normalize the concentrations of Na^+ ions in NOHM-I-HPE-based fluids, a salt content parameter, c, is introduced, which corresponds to the number of moles of salt cation (in this case Na^+) associated with one ether oxygen group in the HPE polymeric canopy (eq 1).

$$c_{NOHMs} = \frac{mass\ Na^+}{mass\ NOHMs} \cdot \frac{MW\ HPE}{MW\ Na^+} \cdot \frac{1\ mol\ HPE}{41\ mol\ O} \cdot \frac{1\ g\ NOHMs}{0.8\ g\ organic} \cdot$$
$$\frac{1\ g\ organic}{0.91\ g\ of\ HPE} \tag{1}$$

In this equation, the ratio of mol O to mol HPE is based on the number of ether functional groups in a single Jeffamine polymer chain (41). The ratio of mass of NOHMs (in grams) to mass of organic content (in grams) is based on the known mass fraction of polymer in NOHMs, which was shown from thermogravimetric analysis data of a previous study to be 80 wt % (with the remaining 20 wt % being the

SiO_2 nanoparticle fraction).[33] Finally, the ratio of mass of the organic (in grams) to mass of HPE (in grams) is included to account for the silane linker molecule. This is calculated based on the molecular weights of the Jeffamine M2070 polymer (MW = 2000) and the silane linker (MW = 202.26), which determines that the polymer chains account for 91% (2000/2202.26) of the total organic fraction (Jeffamine M2070 + silane linker), assuming there is exactly one linker group per polymer chain. To remove the added salt from NaCl-containing solutions of NOHM-I-HPE for subsequent characterization, the samples were dialyzed against deionized water for 48 h (3500 MWCO, Thermo Scientific).

Viscosity Measurements

The dynamic viscosities of the samples were measured at a range of temperatures using a piston-based viscometer (VISCOlab 4000, Cambridge Viscosity−PAC) equipped with a water bath (Julabo F12) for temperature control. The uncertainty in the viscometer measurements was determined to be within ±5% for all samples.

Dynamic Light Scattering

The hydrodynamic diameter (d_H) of NOHM-I-HPE in binary fluids was determined via DLS (Zetasizer Nano ZS, Malvern Panalytical) employing 3.5 mL quartz cuvettes (Cole Parmer) with a path length of 10 mm. The experiments were carried out at 25 °C in dilute aqueous suspensions of 1 wt % NOHM-I-HPE mixtures, and the value reported is the average of three measurements. Samples were passed through a 0.2 μm syringe filter (Thermo Scientific) to remove any dust particles before each measurement.

Pulsed-Field Gradient Nuclear Magnetic Resonance (PFG NMR)

The PFG NMR experiments were carried out on aqueous mixtures of 10 wt % NOHM-I-HPE and various NaCl concentrations between 0 and 0.5 M. The sample compositions are also reported in terms of the salt content defined in eq 1 (moles of Na^+ per mole of O along the polymer chains). The 1D ¹H and PFG NMR measurements were performed using a Bruker Avance III 400 WB spectrometer, operating at 400.13 MHz for protons. A longitudinal eddy current delay bipolar gradient pulse (ledbpgp2s) sequence was used to observe the diffusion coefficient at 25 °C of ¹H nuclei in the water molecule and in the untethered HPE and tethered NOHM-I-HPE canopy. The probe used for the measurements is a broad band probe equipped with a 60 G·cm⁻¹ gradient coil. The signal intensity of NMR spectra depends on the magnetic gradient strengths, which were arrayed in 25 values with linear increments in DOSY experiments.

ROESY (Rotating-Frame Overhauser Effect Spectroscopy) NMR

The 2D ¹H−¹H ROESY NMR spectra were recorded in a phase-sensitive mode with 1024 points in the F^2 dimension and 256 points

in the F^1 dimension with exponential filtration in both dimensions. Mixing time value, τ_m, was 0.29 s. For ^{23}Na diffusion, coefficient measurements were performed at 25 °C with a 300 MHz Varian-S direct drive wide bore spectrometer equipped with a DOTY Scientific Z-Spec gradient probe (DS-1034). In that instrument, ^{1}H and ^{23}Na resonances were centered at 302.7 and 79.9 MHz, respectively. The gradient for each experiment was arrayed with 16 or 32 linearly increasing values. For proton diffusion, the g values ranged from 0 to 100 G/cm, whereas in case of sodium, g ranged from 0 to 700 G/cm. For ^{1}H, the gradient pulse width δ was 2 ms, and for ^{23}Na, $\delta = 1$ ms. The gradient pulse separation Δ was 200 ms for both nuclei. For each experiment, the integrated intensities S as a function of applied gradient g (in T/cm) were obtained. The diffusion coefficients were obtained by plotting the NMR signal intensity versus the gradient strength using Stejskal−Tanner equation, shown in eq 2.

$$I = I_0 \cdot e^{-D(\gamma g \delta)^2 \left(\Delta - \frac{\delta}{3}\right)} \tag{2}$$

where I is the signal intensity of NMR spectra with gradient g applied, I_0 is the signal intensity without gradient g applied, γ is the gyromagnetic ratio of the studied nucleus, δ is the gradient pulse duration, and Δ is the diffusion delay.[47]

Conductivity

The ionic conductivities of the NOHM-based fluids with and without salts were measured at 25 °C using a micro 2 platinum poles conductivity probe (Cond probe InLab 752-6 mm, Mettler Toledo) and a conductivity benchtop meter (S230 SevenCompact Conductivity Meter, Mettler Toledo) with 0.5% accuracy.

■ RESULTS AND DISCUSSION

Effect of Salt Addition on the Viscosity of NOHM-Based Fluids

NOHM-I-HPE-based fluids exhibit a nonlinear increase in viscosity with increasing wt % of NOHM-I-HPE in water, as shown in Figure SI.1. The high solution viscosity becomes particularly apparent above 30 wt % NOHM-I-HPE, where the viscosity surpasses 100 cP, as depicted in Figure 2a. We have previously reported that the viscosity of NOHM-I-HPE-based fluids is significantly higher than that of a solution of the constituent HPE polymer at comparable concentrations, which is attributed to the presence of the inorganic SiO$_2$ nanocores.[34,55] This is in agreement with the literature, and a similar effect has been reported in the case of polymer-grafted nanoparticles due to the increased hydrodynamic size of the grafted nanoparticle units compared to that of untethered polymer solutions, as well as restrictions on the polymer mobility imposed by space-filling requirements.[56−58] This high solution viscosity would severely limit the application of NOHM-based solutions as electrolytes for various electrochemical technologies.

Our recent study has shown that the selection of the secondary fluid (e.g., polar protic, polar aprotic, nonpolar) significantly impacts the apparent viscosities of NOHM-based electrolytes.[59] While there are several options for solvents, the use of water as the secondary fluid is attractive for NOHM-based electrolytes, as it is a low-cost and environmentally safe fluid. As we consider NOHMs as potential additives for novel electrolytes, it is important to understand the interaction between NOHMs and salt and how it would impact the transport properties in electrolytes. Interestingly, as the supporting electrolyte (e.g., NaCl) was added to NOHM solutions, the viscosity of the NOHM-based fluid was significantly reduced (see Figure 2). This behavior suggests that the interaction between NOHMs and the ionic stimulus such as Na$^+$ ions can impact the transport behaviors within

NOHM-based electrolytes. Thus, this study investigated the effect of salt addition (i.e., NaCl) on the transport properties of NOHM-I-HPE solutions.

As presented in Figure 2a, the addition of 0.1 M NaCl to NOHM solutions led to significantly lowered viscosities in all concentration ranges of NOHM-I-HPE studied. Figure 2b summarizes the percentage decrease in the electrolyte viscosity with the addition of 0.1 M NaCl for 10, 20, 30, 40, and 50 wt % NOHM-I-HPE in water. In all cases, the viscosity of the NOHM solution decreases by more than 50% upon the addition of 0.1 M NaCl, and the effect was greater for higher NOHM-I-HPE concentration cases. For instance, the viscosity of 50 wt % NOHM-I-HPE in water was measured to be 785 ± 39 cP at 20 °C, and this was reduced by nearly 90% to 78.9 ± 3.9 cP upon the addition of 0.1 M NaCl. These results suggest that salt addition can be employed as a key parameter to control the viscosity of NOHM-I-HPE-based electrolytes and ultimately enhance charge transport behaviors in these electrolytes.

As seen in Figure 2a, the viscosities of NOHM-I-HPE-based electrolytes, both with and without added NaCl, decreased upon heating. In previous studies, the viscosity−temperature relation for NOHM-I-HPE and water mixtures was modeled with the commonly used Arrhenius equation shown in eq 3.[55]

$$\eta = \eta_\infty e^{-E_a/RT} \tag{3}$$

where η is the viscosity, η_∞ is the viscosity at infinite temperature, R is the universal gas constant, E_a is the activation energy for flow, and T is the temperature. The Arrhenius equation was found to also model the viscosity−temperature relation suitably for NOHM-I-HPE solutions with added NaCl. Plots of the viscosities measured as a function of temperature are shown in Figures SI.2 and SI.3, and the R^2 values and fitting parameters (E_a and η_∞) of each sample are reported in Tables SI.3 and SI.4, respectively.

E_a is generally used as an indication of the difficulty of moving flow units (polymer chain segments) from one position to another and is known to be influenced by the intensity of interchain interactions, chain rigidity, free volume considerations, and polymer hydrodynamic parameters.[60,61] The activation energy for the flow of NOHM-I-HPE solutions was found to be in the range of −18.0 to −20.0 kJ/mol NOHM-I-HPE, which is comparable to the previously reported values.[55] As NaCl was added, the E_a for solutions of NOHM-I-HPE was significantly reduced, and this phenomenon was stronger for lower NOHM-I-HPE concentration cases. For instance, the E_a of 20 wt % NOHM-I-HPE solution was −21.8 kJ/mol, and it was reduced to −16.1 kJ/mol when 0.1 M NaCl was added to the system. Based on the significant decrease in E_a upon salt addition, we hypothesized that the interaction with ionic species may have induced structural changes in the NOHMs' polymeric canopy, favoring chain mobility, an effect that is further explored in subsequent sections.

On the other hand, at NOHM concentrations above 40 wt %, the differences between E_a of NOHM-I-HPE solutions with and without 0.1 M NaCl became negligible. This suggests that other effects impacting polymer mobility might play a role at higher NOHM concentration in solution. As outlined previously, Haque et al. found that there are three different types of polymers exist in NOHM-based fluids—tethered, interacting, and free, making the dynamic behaviors of

NOHMs in water more complex but also tunable.[62] It was found that there was a higher fraction of free and interacting polymers in solution at higher NOHM concentrations,[62] which would impact the overall polymer chain mobility in solution and could account for these differences in E_a trends.

Transition from Ionic Stimuli-Responsive Regime to Saturation Regime

To further probe the effect of salt addition on the viscosity behaviors of NOHM-I-HPE-based electrolytes, a wide range of salt concentrations was explored. A 50 wt % NOHM-I-HPE solution was selected as the basis for this part of the study, as higher NOHM concentrations are desired for electrochemical applications (e.g., increased concentrations of redox-active species in flow batteries). Solutions of 50 wt % NOHM-I-HPE with varying salt concentrations in the range of 0.025 to 1 M NaCl were prepared, and the resulting viscosities at 20, 30, and 40 °C are shown in Figure 3a.

(a)

(b)
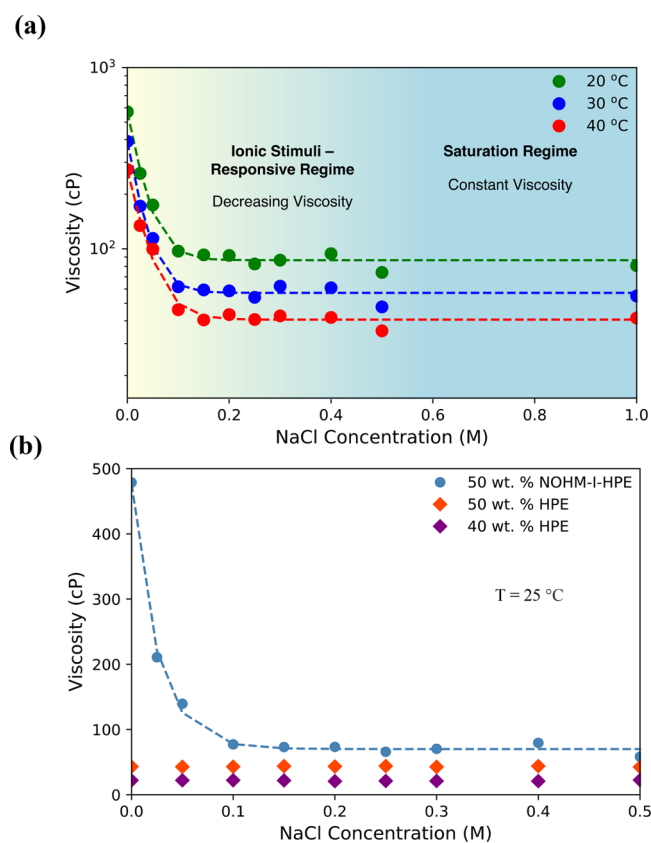
Figure 3. Regime transition in the viscosity behaviors of NOHM-based fluids as a function of salt concentration (NOHMs = HOHM-I-HPE, salt = NaCl) at different temperatures. (a) Viscosity of 50 wt % NOHM-I-HPE solutions with addition of varying NaCl concentrations at 20, 30, and 40 °C. (b) Viscosity of 50 wt % NOHM-I-HPE solutions compared to 50 wt % HPE solution (the same total wt %) and 40 wt % HPE solutions (the same wt % of HPE polymer in solutions) as a function of NaCl concentrations at 25 °C.

A nonmonotonic decrease in viscosity was observed with increasing salt concentration. At 20 °C, the viscosity of 50 wt % NOHM-I-HPE decreased from 570 ± 28 to 260 ± 13 cP with the addition of just 0.025 M NaCl, indicating that a change in electrolyte viscosity can be induced even at a very low salt concentration. As the salt concentration increased, the electrolyte viscosity plateaued at around 0.15 M NaCl addition.

This is now referred to herein as the "critical salt concentration", at which the measured solution viscosity is constant with respect to measurements at higher salt concentrations. Thus, we defined two different viscosity regimes for the unique viscosity behavior of NOHM-based electrolytes in water, as illustrated in Figure 3a. The first regime, observed at low salt concentration, corresponds to an "ionic stimulus-responsive regime", where the measured solution viscosity is found to decrease with increasing ionic strength of the solution. The second regime, observed at higher salt concentrations, is a "saturation regime", where viscosity remains unchanged and becomes unresponsive to increases in solution ionic strength.

As discussed previously, NOHMs' polymeric canopy contains different types of polymers (i.e., tethered, interacting, and free), and their interactions with ionic stimulus and water would impact the viscosity behaviors of NOHM-based fluids. Thus, the changes in viscosity of NOHM-based mixtures were compared to the behaviors of HPE solutions, which only contain free polymers. Figure 3b shows the viscosities of 50 wt % NOHM-I-HPE and 50 wt % HPE in water with varying salt concentrations between 0.025 to 0.5 M NaCl at 25 °C. While the NOHM-based solutions exhibited a significant decrease in solution viscosity, described above, the viscosity of a 50 wt % HPE polymer solution remained unchanged with the addition of NaCl. To compare this behavior at the same polymer loading (excluding SiO_2 nanocores in NOHM-I-HPE) in solution, 40 wt % HPE solutions were also prepared. The viscosities of these solutions with the addition of varying salt concentrations between 0.025 to 0.5 M NaCl are also shown in Figure 3b and show no changes with addition of salt. These results highlight that the polymeric canopy of NOHMs is associated with a different response to changes in ionic strength compared to untethered polymers in solution, an effect that is further explored in the next section.

Our previous study has found that the conformation of the polymeric canopy in NOHM-I-HPE-based electrolytes is dependent on the secondary fluid, with its polarity playing an important role. Thus, we hypothesized that the observed decrease in measured viscosity with the addition of salt could also be attributed to changes in the polymer structural conformation, including the degree of swelling/stretching of the grafted polymeric canopy away from the nanoparticle cores, due to alterations in intermolecular interactions in the system with ionic stimulus. Additionally, the introduction of charged salt ions in the system could disrupt the ionic bond between the nanoparticle and the Jeffamine (HPE) polymer, an effect that has previously been reported by Jespersen and co-workers,[53,62] leading to changes in solution properties.

Changing Structural Configuration of NOHMs' Polymeric Canopy in the Presence of Ionic Stimulus

To investigate the effect of salt addition on the polymeric canopy conformation of NOHMs, DLS was employed. DLS estimates the outermost diameter (hydrodynamic diameter) of a particle based on the speed of particle diffusion, from which size can be determined using the Stokes−Einstein relationship. The mean hydrodynamic diameter (d_H) of NOHM-I-HPE in water at a concentration of 1 wt % was found to be 30.5 ± 3.0 nm. From d_H, the thickness of the polymeric canopy of NOHM-I-HPE in water can be estimated after accounting for the 7 nm SiO_2 core. It was approximately 11.8 nm, which is significantly greater than the radius of gyration of the Jeffamine
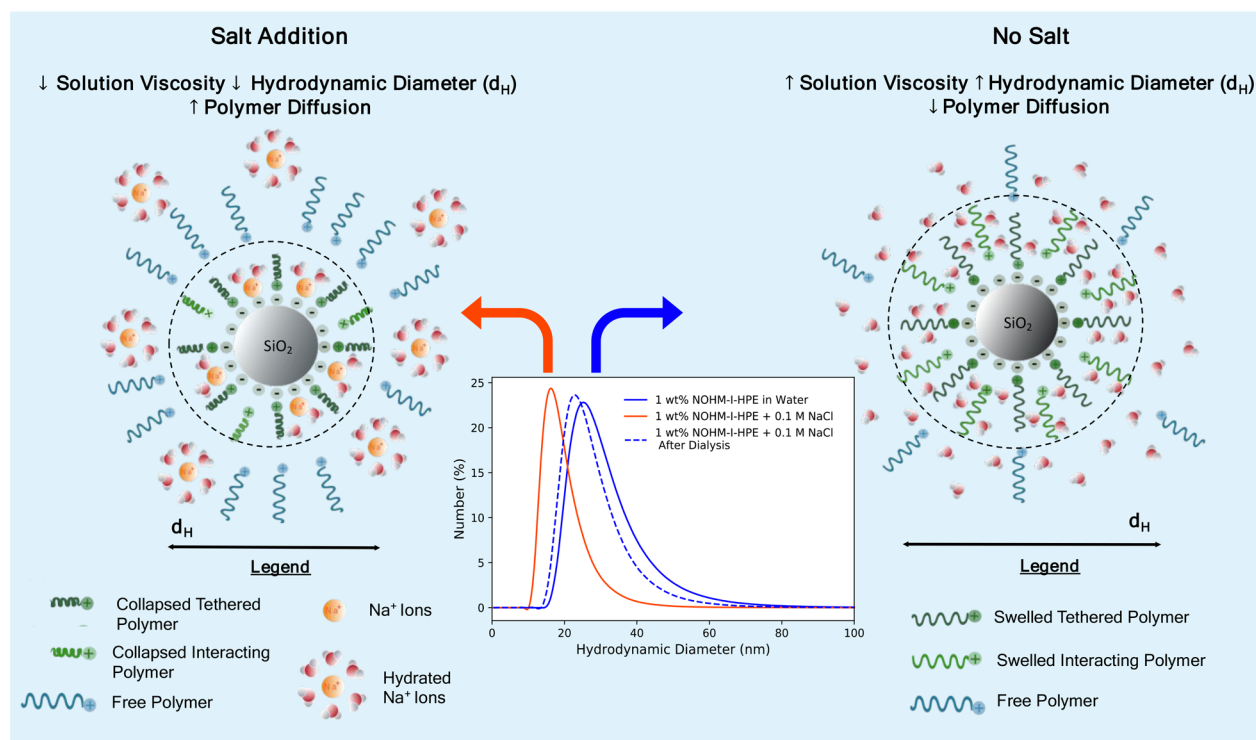
Figure 4. Proposed mechanisms of conformational changes of NOHMs' polymeric canopy in water with salt addition (e.g., NOHMs = NOHM-I-HPE and salt = NaCl). Inset: Number distribution of hydrodynamic diameter of NOHM-I-HPE in water with (orange line) and without (blue line) salt (NaCl) addition. DLS measurements were performed using 1 wt % NOHM-I-HPE in water at 25 °C. Dashed blue line represents the DLS measurement performed after dialysis.

M-2070 polymer (1.25 nm), assuming a freely jointed chain.[63] This agrees with our previous findings on the presence of different layers of polymers (tethered and interacting) in the canopy of NOHMs[62] and also suggests that the intermolecular interactions between the grafted polymer and the solvent induce swelling/stretching of the constituent polymer away from the nanoparticle surface. Swelling of Jeffamine M-2070 on silica particles has also been reported in the literature for liquid polymer nanocomposites.[64]

The inset of Figure 4 shows the hydrodynamic diameter distributions of NOHM-I-HPE in water with and without 0.1 M NaCl. Upon the addition of 0.1 M NaCl, the d_H of NOHMs decreased to 18.4 ± 0.3 nm, estimating the thickness of the polymeric canopy to be 5.7 nm. This decrease in d_H could be attributed to two potential effects. The first is a reduction of the extent of polymer swelling induced by the introduction of Na$^+$ ions, disrupting the hydrogen bonding network between water and the polymeric canopy that is present in the absence of salt. The second is a decrease in ability of the interacting polymer layer to penetrate the tethered polymer due to the Na$^+$ ions effectively screening some of the charges on the nanoparticle surface. This has been reported for systems of NOHM-I-HPE at higher wt % with added salt (KHCO$_3$), where SANS measurements showed an increase in the effective thickness of the tethered polymer layer with added salt in solution.[62] These findings are consistent with the DLS measurements presented here, where the system previously shown to have a greater fraction of interacting polymer displayed a greater effective hydrodynamic diameter.[62] This second effect could also contribute to the first, as the reduction of polymer crowding around the nanoparticle with decreased penetration of the interacting polymer layer would reduce

steric hindrance of the grafted polymer brushes, potentially leading to their collapse into a "mushroom-like" rather than "rod-like" configuration.[65] The absence of additional peaks in the cases with and without salt suggest that no particle aggregation is present at this concentration. Figure 4 illustrates the presence of different polymers in NOHM-based fluid systems and the changes in d_H with the addition of ionic stimulus.

To study the reversibility of the structural configuration of ionically tethered polymers in NOHMs, a dilute NOHM-I-HPE mixture in 0.1 M NaCl was dialyzed (3500 MWCO) against deionized water for 48 h to remove NaCl. The dashed line in Figure 4 represents the hydrodynamic diameter distribution of the dialyzed NOHM-I-HPE mixture, and the mean hydrodynamic diameter was 25.6 ± 0.5 nm. This suggests that upon the removal of salt ions via dialysis, the constituent NOHMs' polymeric canopy starts to interact with the water solvent and swells, approaching its initial d_H measured without adding NaCl. This highlights the reversibility of the polymer conformational changes induced by an ionic stimulus. The slight difference between the hydrodynamic diameter distributions of NOHM-I-HPE in water (without salt) and in water after dialysis is attributed to not all the added salt being completely removed. This is consistent with previous studies that have found that ionic contaminants are difficult to completely remove from NOHMs.[53,56,66]

DLS was also employed to investigate the effect of salt addition on the hydrodynamic size of the untethered HPE polymer in water. The mean hydrodynamic diameter of HPE in water was found to be 2.1 ± 0.1 nm. Upon adding 0.1 M NaCl, the measured hydrodynamic diameter was 2.6 ± 0.2 nm. Table 1 summarizes the effect of 0.1 M NaCl addition on the

Table 1. Hydrodynamic Diameters of NOHM-I-HPE and HPE in Water Measured via DLS at 25 °C

solution	measured d_H, no NaCl	measured d_H, 0.1 M NaCl
1 wt % NOHM-I-HPE in water	30.5 ± 3.0 nm	18.4 ± 0.3 nm
1 wt % HPE in water	2.1 ± 0.1 nm	2.6 ± 0.2 nm

hydrodynamic diameter of HPE, and their behaviors are compared to those of NOHM-I-HPE. While NOHM-I-HPE underwent significant decrease of its hydrodynamic diameter with the addition of NaCl, as previously discussed, the measured size of HPE remained nearly unchanged. This is consistent with the difference in bulk behaviors of NOHM-I-HPE and HPE, described in the previous section.

In an attempt to explicitly identify interactions between components (i.e., HPE, water, and NaCl), Figure 5a shows a representative ROESY NMR spectra for 50 wt % NOHM-I-HPE in water with 0.1 M NaCl. The homonuclear NMR spectroscopic technique using 2D ROESY employs a second frequency dimension based on the nuclear Overhauser enhancement effect in which correlations are seen between spatially proximal and chemically exchanging spins. The sign of the ROESY, indicated by colors in Figure 5 (blue and red represent negative and positive, respectively), can provide key information for the interpretation: ROESY cross-peaks would be negative (relative to the phase of the diagonal) if they arise from direct dipolar interactions (the ROE), whereas those cross-peaks stemming from spin diffusion (a three-spin effect or a relayed ROE) would be positive. TOCSY (total correlated spectroscopy) cross-peaks, which arise from J-coupled spin systems, can also be observed in many ROESY spectra, but the sign of these cross-peaks is positive.[67]

To analyze the ROESY spectrum, it is necessary to interpret the 1D NMR spectrum (Figure SI.4) first. The main features in the 1D NMR spectrum (Figure SI.4) correspond to the water peak at 4.5 ppm, the methyl group at 1.0 ppm (peak b) from the propylene oxide, the peaks at 3.51 and 3.35 (peak d) assigned to the methylene protons from ethylene oxide, and

the peak at 3.2 ppm (peak a) assigned to the terminal methyl attached to ethylene oxide. In general, all samples regardless of salt content, exhibited ROESY cross-peaks between the water peak and peaks b and d, associated with the methyl group from propylene oxide and methylene groups from ethylene oxide. A cross-peak indicating interchain interaction can also be observed, suggesting interaction between the methyl group in propylene oxide and the methylene groups in ethylene oxide (b–d). The integral intensity of the cross-peaks was estimated using the integral intensity of the water diagonal peak as a reference (Table SI.8). The ratio between the cross-peak and the diagonal peak integral can be used to indicate the internuclear distance.[68]

The comparison of the estimated ratio for the 50 wt % NOHM-I-HPE in water in the absence of ($1.46 \times 10^{-2} \pm 0.2 \times 10^{-2}$) and in the presence of NaCl ($2.03 \times 10^{-2} \pm 0.2 \times 10^{-2}$) suggests a larger interproton distance between the solvent and the methylene groups in the polymeric canopy when salt is present. This suggests that the water molecules present in the polymeric canopy are hydrating the Na^+ ions when salt is present, decreasing the tendency for water to H-bond with the etheric oxygen. This is consistent with the relatively weak H-bonding interaction relative to ion hydration.[69] The loose H-bonded water network structure present without salt, responsible for the swelling of the polymeric canopy, therefore collapses in the presence of salt with Na^+ ions breaking up this network as they become hydrated. This is also supported by findings of the DLS measurements described in the previous section. These ROESY NMR measurements provided insights into the alterations in intermolecular interactions between the polymeric canopy of NOHMs and the surrounding water molecules upon the addition of Na^+ ions in the system.

Diffusion NMR experiments were also carried out to study the effect of salt addition on the mobility of NOHM-I-HPE and HPE in water. The self-diffusion coefficient was estimated from the intensities of the peaks related to the HPE and NOHM-I-HPE polymer canopy as a function of NaCl content. Figure 5b presents the behavior of the self-diffusion coefficient
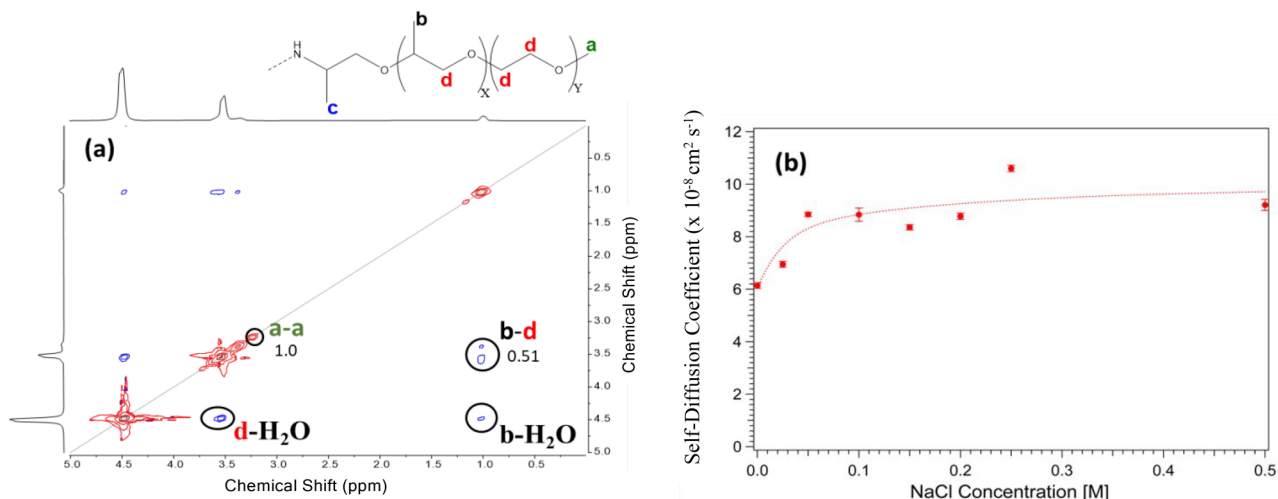
Figure 5. Effect of salt addition on structures and dynamics of NOHM-I-HPE in water. (a) 2D $^1H-^1H$ ROESY NMR spectrum of 50 wt % NOHM-I-HPE in water with 0.1 M NaCl. The red contours correspond to diagonal and TOCSY (total correlation spectroscopy, off-diagonal) peaks, and the blue contours exhibit ROEs. The diagonal peak used to standardize the integration has been circled along with the cross-peak. The letters indicate the interacting protons, and the numbers indicate the integrated intensities. The mixing time is $\tau_m = 0.2$ s; $T = 25$ °C. (b) ^1H self-diffusion coefficients of 50 wt % NOHM-I-HPE canopy protons as a function of NaCl concentration at 25 °C.

of the polymer canopy in NOHM-I-HPE as a function of salt concentration. The diffusion coefficient of the canopy protons in the NOHM-I-HPE (D_{NP}) exhibited an increase as NaCl was added. The data suggest that a plateau was reached at a concentration of approximately 0.1 M NaCl, which agreed with the transition to the "saturation regime" identified in Figure 3. The estimated diffusion coefficient of free HPE in water (D_P), on the other hand, did not show dependency on the NaCl content, which is also consistent with the results presented in the previous sections (Figure SI.5).

Together, the DLS and NMR measurements therefore suggest that the two potential effects outlined in Figure 4 are both occurring in the NOHMs' polymeric canopy upon the addition of supporting electrolyte (e.g., NaCl). First, the addition of Na^+ disrupted the H-bonding network between the etheric functional groups along the polymer chains and the secondary fluid (water) due to the hydration of the Na^+ ions, which led to a collapse of the polymeric canopy of NOHMs in water. Additionally, the introduction of Na^+ ions reduced the ability of interacting polymer to penetrate the tethered polymer layer of NOHMs. The observed dramatic decrease in solution viscosity shown in Figure 3 can be related to both of these effects, and these behaviors are graphically illustrated in Figure 4.

Ionic Mobility and Conductivity of NOHM-Based Electrolytes

The effect of ionic stimulus on the bulk properties of NOHM solutions and the structural configuration of the polymeric canopy suggest that NOHM-based fluids can be designed and tailored to be effective electrolytes. To further investigate the mechanisms of salt effect on NOHM-based electrolytes, the interactions between Na^+ and different components of NOHM-based solution were studied. This includes Na^+ that may be interacting with the charged nanoparticle surface (and also potentially with the polymeric canopy) and is effectively "trapped" within the polymeric canopy. Na^+ ions also exist in the bulk solution in hydrated form. The study of the conduction pathways and exchange within these Na^+ in different locations (within the polymeric canopy versus bulk fluid) was important, as they would directly impact transport properties in NOHM-based electrolyte systems. Thus, ^{23}Na diffusion measurements were performed to obtain insights into the mobility of Na^+ ions within the NOHM-I-HPE-based electrolytes.

Figure 6 shows the self-diffusion coefficients of Na^+ in 10 wt % NOHM-I-HPE solutions with varying concentrations of added NaCl (an example of the ^{23}Na NMR spectra is given in Figure SI.6), and the results are compared to the viscosity changes (red data set). The salt concentration is given as the salt content defined in eq 1. At the lowest salt contents (<0.01 Na/O), the Na^+ is found to be much less mobile, implying that it is largely trapped within the canopy of the NOHMs. As the salt content increases, the Na^+ diffusion coefficient rises fairly sharply up to 0.15 Na/O salt content. This phenomenon may be related to the reduced number of interacting polymers within the NOHMs' canopy layer as well as the reduced hydrodynamic diameter of NOHMs at higher salt contents, as illustrated in Figure 4. These structural changes within the NOHMs' polymeric canopy would have improved the mobility of the Na^+ trapped within it. As the salt content continues to increase, a greater fraction of the Na^+ ions would be in the bulk solution, hence the diffusion coefficient rises gradually,
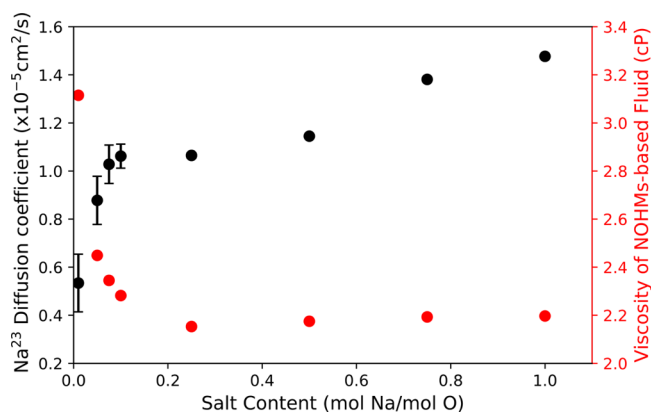
Figure 6. ^{23}Na self-diffusion coefficients measured in 10 wt % NOHM-I-HPE solutions, as a function of ratio between salt and NOHMs' polymeric functional groups (i.e., ether (O)) (mol Na/mol O) at 25 °C. The error bars of diffusion coefficients are associated with a signal-to-noise ratio of the spectra, which was negligible at higher salt concentrations.

approaching the diffusion coefficient of NaCl measured in dilute aqueous solution.[70]

Proton diffusion measurements were also performed on the 10 wt % NOHM-I-HPE solutions. Protons from NOHM ether groups as well as water molecules were present. In the 1D NMR spectrum, we clearly see two peaks—the lower intensity peak near 0 ppm was the NOHM contribution. A representative spectrum is displayed in Figure SI.6. The water proton diffusion data did not exhibit a clear trend with increased salt concentrations as the Na data, suggesting that, at this NOHM concentration (10 wt %), water molecular motion was not sufficiently impacted.

Next, to evaluate NOHM-based fluids as electrolytes, we performed conductivity measurements, and the data were compared with previously reported conductivity and viscosity data for other novel electrolytes employed in electrochemical applications, such as ILs and DES. Figure 7 shows the measured conductivity and viscosity of 50 wt % NOHM-I-HPE mixtures with varying NaCl concentrations between 0.05 and 0.5 M. The detailed data are reported in Table SI.11. It is
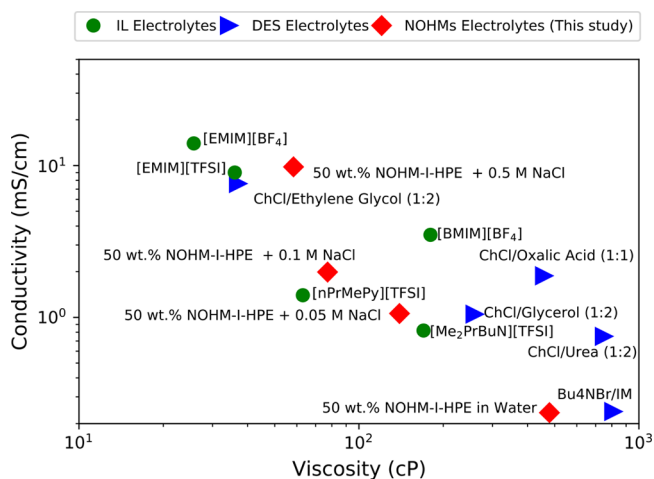
Figure 7. Conductivity and viscosity of NOHM-based electrolytes for electrochemical energy storage applications. Data measured at 25 °C and compared to conductivity and viscosity of deep eutectic solvents[26−28] and ionic liquids[25] that were also measured at 25 °C.

evident from Figure 7 that the addition of salt (NaCl) reduced the viscosity of NOHM-based electrolyte, while significantly increasing its conductivity by an order of magnitude. A 50 wt % NOHM-I-HPE solution with 0.5 M NaCl showed promising results as an electrolyte, comparable to ILs and DESs, which achieved conductivities in the range of 0.1 to 10 mS/cm.[25−28] A 50 wt % NOHM-I-HPE solution in water, for example, showed a conductivity of 0.2 mS/cm at 25 °C.

It should be noted that the conductivities of these novel electrolytes including ILs, DES, and NOHM-based fluids are still significantly lower than that of conventional aqueous electrolytes employed in electrochemical applications.[71] NaCl (2 M) in water, for example, has an ionic conductivity of 145 mS/cm.[71] However, NOHM-based electrolytes as well as ILs and DESs have the potential to greatly improve the solubilities of reactants (e.g., CO_2 and redox-active species) in the solution compared to conventional electrolytes. Thus, a more in-depth study is desired to understand how the chemical and structural changes of these complex fluids can enhance their charge transport behaviors to make them effective for electrochemical systems. In particular, it is evident that from this work that the addition of salt is an important parameter for controlling the transport properties of NOHM-based electrolytes.

CONCLUSIONS

This study showed that salt addition is a critical parameter to tune the transport properties of NOHM-I-HPE-based electrolytes. Up to 90% viscosity reduction was achieved with the addition of 0.1 M NaCl to NOHM-I-HPE-based solutions. Dynamic light scattering, NMR diffusion, and ROESY NMR measurements suggest that the structural configuration of the polymeric canopy (including both tethered and interacting polymers) was significantly impacted by changes in the ionic strength of the solution. Two different mechanisms were proposed to explain the drastic viscosity reduction in NOHM-based solutions. The first was the disruption of intermolecular interactions, in particular, H-bonding, between the ether-containing polymeric canopy and the surrounding water, due to hydration of the salt ions (Na^+), leading to a collapse of the polymeric canopy. The second was the reduced ability of "interacting polymer" to penetrate the tethered polymer layer of NOHMs. The findings suggest both of these mechanisms are occurring simultaneously, leading to changes in conformation of the polymeric canopy (both tethered and interacting polymer), which can explain the changes in bulk transport properties observed. The structural changes of NOHMs' polymeric canopy induced by salt addition were found to be reversible. These behaviors of NOHMs were distinct from those of untethered HPE solution, which showed no variations in solution viscosity with increasing NaCl concentrations, as well as no size changes upon increasing ionic strength. The fundamental understanding of changes in polymeric canopy configurations with addition of ionic stimulus in NOHM-based electrolytes revealed by this study provides a capability to tune their intermolecular interactions. This is a promising pathway to overcome challenges associated with the high viscosities of these fluids and significantly improve transport properties which are critical in electrochemical applications, such as batteries and electrochemical CO_2 conversion. Studies are underway to explore the effects of ions of different valences, ionic radii, and binding affinities toward functional groups in the NOHM polymer chains, which

could also offer a new dimension to tailor physicochemical properties of NOHM-based electrolytes.

ASSOCIATED CONTENT

Supporting Information

The Supporting Information is available free of charge at https://pubs.acs.org/doi/10.1021/jacsau.1c00410.

Viscosity of NOHM-I-HPE and HPE solutions at different temperatures with and without addition of NaCl, Arrhenius fits to viscosity data of NOHM-I-HPE and HPE solutions at different temperatures and R^2 values of Arrhenius exponential fits, ^1H NMR spectra and self-diffusion coefficients of NOHM-I-HPE and HPE canopy protons in solution with NaCl addition, ^{23}Na NMR spectra and Na^+ self-diffusion coefficients in NOHM-I-HPE solutions with NaCl addition, ionic conductivity of NOHM-I-HPE solutions with NaCl addition, integration of cross-peaks from $^1H-^1H$ ROESY NMR spectrum (PDF)

AUTHOR INFORMATION

Corresponding Author

Ah-Hyung Alissa Park − *Department of Earth and Environmental Engineering, Columbia University, New York, New York 10027, United States; Department of Chemical Engineering and Lenfest Center for Sustainable Energy, The Earth Institute, Columbia University, New York, New York 10027, United States;* orcid.org/0000-0002-6482-3589; Email: ap2622@columbia.edu

Authors

Sara T. Hamilton − *Department of Earth and Environmental Engineering, Columbia University, New York, New York 10027, United States; Lenfest Center for Sustainable Energy, The Earth Institute, Columbia University, New York, New York 10027, United States*

Tony G. Feric − *Department of Chemical Engineering and Lenfest Center for Sustainable Energy, The Earth Institute, Columbia University, New York, New York 10027, United States;* orcid.org/0000-0001-5608-570X

Sahana Bhattacharyya − *Hunter College Physics Department, City University of New York, New York, New York 10065, United States*

Nelly M. Cantillo − *Department of Chemical & Biomolecular Engineering, The University of Tennessee Knoxville, Knoxville, Tennessee 37996, United States;* orcid.org/0000-0002-9616-4135

Steven G. Greenbaum − *Hunter College Physics Department, City University of New York, New York, New York 10065, United States;* orcid.org/0000-0001-5497-5274

Thomas A. Zawodzinski − *Department of Chemical & Biomolecular Engineering, The University of Tennessee Knoxville, Knoxville, Tennessee 37996, United States; Oak Ridge National Laboratory, Oak Ridge, Tennessee 37830, United States;* orcid.org/0000-0002-2690-8784

Complete contact information is available at:
https://pubs.acs.org/10.1021/jacsau.1c00410

Notes

The authors declare no competing financial interest.

REFERENCES

(1) Dunn, B.; Kamath, H.; Tarascon, J. M. Electrical Energy Storage for the Grid: A Battery of Choices. *Science (80-.)* **2011**, *334* (6058), 928−935.

(2) Trahey, L.; Brushett, F. R.; Balsara, N. P.; Ceder, G.; Cheng, L.; Chiang, Y. M.; Hahn, N. T.; Ingram, B. J.; Minteer, S. D.; Moore, J. S.; et al. Energy Storage Emerging: A Perspective from the Joint Center for Energy Storage Research. *Proc. Natl. Acad. Sci. U. S. A.* **2020**, *117* (23), 12550−12557.

(3) Nitopi, S.; Bertheussen, E.; Scott, S. B.; Liu, X.; Engstfeld, A. K.; Horch, S.; Seger, B.; Stephens, I. E. L.; Chan, K.; Hahn, C.; et al. Progress and Perspectives of Electrochemical CO_2 Reduction on Copper in Aqueous Electrolyte. *Chem. Rev.* **2019**, *119*, 7610−7672.

(4) Amanchukwu, C. V. The Electrolyte Frontier: A Manifesto. *Joule* **2020**, *4*, 281−285.

(5) Wei, X.; Pan, W.; Duan, W.; Hollas, A.; Yang, Z.; Li, B.; Nie, Z.; Liu, J.; Reed, D.; Wang, W.; et al. Materials and Systems for Organic Redox Flow Batteries: Status and Challenges. *ACS Energy Lett.* **2017**, *2* (9), 2187−2204.

(6) Chakrabarti, M. H.; Mjalli, F. S.; Alnashef, I. M.; Hashim, M. A.; Hussain, M. A.; Bahadori, L.; Low, C. T. J. Prospects of Applying Ionic Liquids and Deep Eutectic Solvents for Renewable Energy Storage by Means of Redox Flow Batteries. *Renew. Sustain. Energy Rev.* **2014**, *30*, 254−270.

(7) Chen, Y.; Mu, T. Conversion of CO_2 to Value Added Products Mediated by Ionic Liquids. *Green Chem.* **2019**, *21*, 2544.

(8) Lim, H. K.; Kim, H. The Mechanism of Room-Temperature Ionic-Liquid-Based Electrochemical CO_2 Reduction: A Review. *Molecules* **2017**, *22* (4), 536.

(9) Huang, Z.; Kay, C. W. M.; Kuttich, B.; Rauber, D.; Kraus, T.; Li, H.; Kim, S.; Chen, R. An "Interaction-Mediating" Strategy towards Enhanced Solubility and Redox Properties of Organics for Aqueous Flow Batteries. *Nano Energy* **2020**, *69*, 104464.

(10) Ejigu, A.; Greatorex-Davies, P. A.; Walsh, D. A. Room Temperature Ionic Liquid Electrolytes for Redox Flow Batteries. *Electrochem. commun.* **2015**, *54*, 55−59.

(11) Gurkan, B.; Squire, H.; Pentzer, E. Metal-Free Deep Eutectic Solvents: Preparation, Physical Properties, and Significance. *J. Phys. Chem. Lett.* **2019**, *10* (24), 7956−7964.

(12) Vasilyev, D. V.; Rudnev, A. V.; Broekmann, P.; Dyson, P. J. A General and Facile Approach for the Electrochemical Reduction of Carbon Dioxide Inspired by Deep Eutectic Solvents. *ChemSusChem* **2019**, *12* (8), 1635−1639.

(13) Zhang, C.; Zhang, L.; Ding, Y.; Guo, X.; Yu, G. Eutectic Electrolytes for High-Energy-Density Redox Flow Batteries. *ACS Energy Lett.* **2018**, *3* (12), 2875−2883.

(14) Zhang, L.; Zhang, C.; Ding, Y.; Ramirez-Meyers, K.; Yu, G. A Low-Cost and High-Energy Hybrid Iron-Aluminum Liquid Battery Achieved by Deep Eutectic Solvents. *Joule* **2017**, *1* (3), 623−633.

(15) Montoto, E. C.; Nagarjuna, G.; Hui, J.; Burgess, M.; Sekerak, N. M.; Hernández-Burgos, K.; Wei, T. S.; Kneer, M.; Grolman, J.; Cheng, K. J.; et al. Redox Active Colloids as Discrete Energy Storage Carriers. *J. Am. Chem. Soc.* **2016**, *138* (40), 13230−13237.

(16) Montoto, E. C.; Nagarjuna, G.; Moore, J. S.; Rodríguez-López, J. Redox Active Polymers for Non-Aqueous Redox Flow Batteries: Validation of the Size-Exclusion Approach. *J. Electrochem. Soc.* **2017**, *164* (7), A1688−A1694.

(17) Burgess, M.; Moore, J. S.; Rodríguez-López, J. Redox Active Polymers as Soluble Nanomaterials for Energy Storage. *Acc. Chem. Res.* **2016**, *49* (11), 2649−2657.

(18) Burgess, M.; Hernández-Burgos, K.; Schuh, J. K.; Davila, J.; Montoto, E. C.; Ewoldt, R. H.; Rodríguez-López, J. Modulation of the Electrochemical Reactivity of Solubilized Redox Active Polymers via Polyelectrolyte Dynamics. *J. Am. Chem. Soc.* **2018**, *140* (6), 2093−2104.

(19) Winsberg, J.; Muench, S.; Hagemann, T.; Morgenstern, S.; Janoschka, T.; Billing, M.; Schacher, F. H.; Hauffman, G.; Gohy, J. F.; Hoeppener, S.; et al. Polymer/Zinc Hybrid-Flow Battery Using Block Copolymer Micelles Featuring a TEMPO Corona as Catholyte. *Polym. Chem.* **2016**, *7* (9), 1711−1718.

(20) Lai, Y. Y.; Li, X.; Zhu, Y. Polymeric Active Materials for Redox Flow Battery Application. *ACS Appl. Polym. Mater.* **2020**, *2*, 113−128.

(21) Goeltz, J. C.; Matsushima, L. N. Metal-Free Redox Active Deep Eutectic Solvents. *Chem. Commun.* **2017**, *53* (72), 9983−9985.

(22) Sinclair, N. S.; Poe, D.; Savinell, R. F.; Maginn, E. J.; Wainright, J. S. A Nitroxide Containing Organic Molecule in a Deep Eutectic Solvent for Flow Battery Applications. *J. Electrochem. Soc.* **2021**, *168* (2), 020527.

(23) Ortiz-Martínez, V. M.; Gómez-Coma, L.; Pérez, G.; Ortiz, A.; Ortiz, I. The Roles of Ionic Liquids as New Electrolytes in Redox Flow Batteries. *Sep. Purif. Technol.* **2020**, *252*, 117436.

(24) Soloveichik, G. L. Flow Batteries: Current Status and Trends. *Chem. Rev.* **2015**, *115* (20), 11533−11558.

(25) Osada, I.; De Vries, H.; Scrosati, B.; Passerini, S. Ionic-Liquid-Based Polymer Electrolytes for Battery Applications. *Angew. Chemie - Int. Ed.* **2016**, *55* (2), 500−513.

(26) Zhang, Q.; De Oliveira Vigier, K.; Royer, S.; Jérôme, F. Deep Eutectic Solvents: Syntheses, Properties and Applications. *Chem. Soc. Rev.* **2012**, *41* (21), 7108−7146.

(27) Bahadori, L.; Chakrabarti, M. H.; Mjalli, F. S.; Alnashef, I. M.; Manan, N. S. A.; Hashim, M. A. Physicochemical Properties of Ammonium-Based Deep Eutectic Solvents and Their Electrochemical Evaluation Using Organometallic Reference Redox Systems. *Electrochim. Acta* **2013**, *113*, 205−211.

(28) Abbott, A. P.; Boothby, D.; Capper, G.; Davies, D. L.; Rasheed, R. K. Deep Eutectic Solvents Formed between Choline Chloride and Carboxylic Acids: Versatile Alternatives to Ionic Liquids. *J. Am. Chem. Soc.* **2004**, *126* (29), 9142−9147.

(29) Crosthwaite, J. M.; Muldoon, M. J.; Dixon, J. K.; Anderson, J. L.; Brennecke, J. F. Phase Transition and Decomposition Temperatures, Heat Capacities and Viscosities of Pyridinium Ionic Liquids. *J. Chem. Thermodyn.* **2005**, *37* (6), 559−568.

(30) Izgorodina, E. I.; Maganti, R.; Armel, V.; Dean, P. M.; Pringle, J. M.; Seddon, K. R.; MacFarlane, D. R. Understanding the Effect of the C2 Proton in Promoting Low Viscosities and High Conductivities in Imidazolium-Based Ionic Liquids: Part I. Weakly Coordinating Anions. *J. Phys. Chem. B* **2011**, *115* (49), 14688−14697.

(31) Tsunashima, K.; Sugiya, M. Physical and Electrochemical Properties of Low-Viscosity Phosphonium Ionic Liquids as Potential Electrolytes. *Electrochem. commun.* **2007**, *9* (9), 2353−2358.

(32) Zhu, J.; Yu, K.; Zhu, Y.; Zhu, R.; Ye, F.; Song, N.; Xu, Y. Physicochemical Properties of Deep Eutectic Solvents Formed by Choline Chloride and Phenolic Compounds at T = (293.15 to 333.15) K: The Influence of Electronic Effect of Substitution Group. *J. Mol. Liq.* **2017**, *232*, 182−187.

(33) Lin, K.-Y. A.; Park, A. H. A. Effects of Bonding Types and Functional Groups on CO₂ Capture Using Novel Multiphase Systems of Liquid-like Nanoparticle Organic Hybrid Materials. *Environ. Sci. Technol.* 2011, 45 (15), 6633–6639.

(34) Petit, C.; Lin, K.-Y. A.; Park, A.-H. A. Design and Characterization of Liquidlike POSS-Based Hybrid Nanomaterials Synthesized via Ionic Bonding and Their Interactions with CO₂. *Langmuir* 2013, 29 (39), 12234–12242.

(35) Andrew Lin, K.-Y.; Park, Y.; Petit, C.; Park, A.-H. A. Thermal Stability, Swelling Behavior and CO₂ Absorption Properties of Nanoscale Ionic Materials (NIMs). *RSC Adv.* 2014, 4 (110), 65195–65204.

(36) Khurana, R.; Schaefer, J. L.; Archer, L. A.; Coates, G. W. Suppression of Lithium Dendrite Growth Using Cross-Linked Polyethylene/Poly(Ethylene Oxide) Electrolytes: A New Approach for Practical Lithium-Metal Polymer Batteries. *J. Am. Chem. Soc.* 2014, 136 (20), 7395–7402.

(37) Tikekar, M. D.; Archer, L. A.; Koch, D. L. Stability Analysis of Electrodeposition across a Structured Electrolyte with Immobilized Anions. *J. Electrochem. Soc.* 2014, 161 (6), A847–A855.

(38) Lu, Y.; Das, S. K.; Moganty, S. S.; Archer, L. A. Ionic Liquid-Nanoparticle Hybrid Electrolytes and Their Application in Secondary Lithium-Metal Batteries. *Adv. Mater.* 2012, 24 (32), 4430–4435.

(39) Schaefer, J. L.; Moganty, S. S.; Yanga, D. A.; Archer, L. A. Nanoporous Hybrid Electrolytes. *J. Mater. Chem.* 2011, 21 (27), 10094–10101.

(40) Schaefer, J. L.; Moganty, S. S.; Archer, L. A. Nanoscale Organic Hybrid Electrolytes. *Adv. Mater.* 2010, 22 (33), 3677–3680.

(41) Lin, K.-Y. A.; Petit, C.; Park, A.-H. A. Effect of SO2 on CO₂ Capture Using Liquid-like Nanoparticle Organic Hybrid Materials. *Energy Fuels* 2013, 27 (8), 4167–4174.

(42) Park, Y.; Decatur, J.; Lin, K. Y. A.; Park, A. H. A. Investigation of CO₂ Capture Mechanisms of Liquid-like Nanoparticle Organic Hybrid Materials via Structural Characterization. *Phys. Chem. Chem. Phys.* 2011, 13 (40), 18115–18122.

(43) Park, Y.; Petit, C.; Han, P.; Alissa Park, A.-H. H. Effect of Canopy Structures and Their Steric Interactions on CO₂ Sorption Behavior of Liquid-like Nanoparticle Organic Hybrid Materials. *RSC Adv.* 2014, 4 (17), 8723–8726.

(44) Mapesa, E. U.; Cantillo, N. M.; Hamilton, S. T.; Harris, M. A.; Zawodzinski, T. A.; Alissa Park, A. H.; Sangoro, J. Localized and Collective Dynamics in Liquid-like Polyethylenimine- Based Nanoparticle Organic Hybrid Materials. *Macromolecules* 2021, 54, 2296.

(45) Cantillo, N. M.; Bruce, M.; Hamilton, S. T.; Feric, T. G.; Park, A.-H. A.; Zawodzinski, T. Electrochemical Behavior of Copper Ion Complexed with Nanoparticle Organic Hybrid Materials. *J. Electrochem. Soc.* 2020, 167, 116508.

(46) Yu, W.; Wang, T.; Park, A. H. A.; Fang, M. Review of Liquid Nano-Absorbents for Enhanced CO₂ Capture. *Nanoscale* 2019, 11 (37), 17137–17156.

(47) Overa, S.; Feric, T. G.; Park, A. H. A.; Jiao, F. Tandem and Hybrid Processes for Carbon Dioxide Utilization. *Joule* 2021, 5 (1), 8–13.

(48) Wang, D.; Yu, W.; Gao, M.; Liu, K.; Wang, T.; Park, A.; Lin, Q. A 3D Microfluidic Device for Carbon Capture Microcapsules Production. In *Proceedings of the IEEE International Conference on Micro Electro Mechanical Systems*, 2018; DOI: 10.1109/MEMSYS.2018.8346776.

(49) Yu, W.; Wang, T.; Park, A.-H. A.; Fang, M. Toward Sustainable Energy and Materials: CO₂ Capture Using Microencapsulated Sorbents. *Ind. Eng. Chem. Res.* 2020, 59, 9746.

(50) Rim, G.; Feric, T. G.; Moore, T.; Park, A. H. A. Solvent Impregnated Polymers Loaded with Liquid-Like Nanoparticle Organic Hybrid Materials for Enhanced Kinetics of Direct Air Capture and Point Source CO₂ Capture. *Adv. Funct. Mater.* 2021, 31, 2010047.

(51) Yu, W.; Wang, T.; Park, A.-H. A.; Fang, M. Toward Sustainable Energy and Materials: CO₂ Capture Using Microencapsulated Sorbents. *Ind. Eng. Chem. Res.* 2020, 59 (21), 9746–9759.

(52) Darling, R. M.; Gallagher, K. G.; Kowalski, J. A.; Ha, S.; Brushett, F. R. Pathways to Low-Cost Electrochemical Energy Storage: A Comparison of Aqueous and Nonaqueous Flow Batteries. *Energy Environ. Sci.* 2014, 7 (11), 3459–3477.

(53) Jespersen, M. L.; Mirau, P. A.; Von Meerwall, E. D.; Koerner, H.; Vaia, R. A.; Fernandes, N. J.; Giannelis, E. P. Hierarchical Canopy Dynamics of Electrolyte-Doped Nanoscale Ionic Materials. *Macromolecules* 2013, 46 (24), 9669–9675.

(54) Petit, C.; Park, Y.; Lin, K.-Y. A.; Park, A.-H. A. Spectroscopic Investigation of the Canopy Configurations in Nanoparticle Organic Hybrid Materials of Various Grafting Densities during CO₂ Capture. *J. Phys. Chem. C* 2012, 116 (1), 516–525.

(55) Petit, C.; Bhatnagar, S.; Park, A. H. A. Effect of Water on the Physical Properties and Carbon Dioxide Capture Capacities of Liquid-like Nanoparticle Organic Hybrid Materials and Their Corresponding Polymers. *J. Colloid Interface Sci.* 2013, 407, 102–108.

(56) Rodriguez, R.; Herrera, R.; Bourlinos, A. B.; Li, R.; Amassian, A.; Archer, L. A.; Giannelis, E. P. The Synthesis and Properties of Nanoscale Ionic Materials. *Appl. Organomet. Chem.* 2010, 24 (8), 581–589.

(57) Kim, S. A.; Mangal, R.; Archer, L. A. Relaxation Dynamics of Nanoparticle-Tethered Polymer Chains. *Macromolecules* 2015, 48 (17), 6280–6293.

(58) Wichaita, W.; Kim, Y. G.; Tangboriboonrat, P.; Thérien-Aubin, H. Polymer-Functionalized Polymer Nanoparticles and Their Behaviour in Suspensions. *Polym. Chem.* 2020, 11 (12), 2119–2128.

(59) Feric, T. G.; Hamilton, S. T.; Cantillo, N. M.; Imel, A. E.; Zawodzinski, T. A.; Park, A.-H. A. Dynamic Mixing Behaviors of Ionically Tethered Polymer Canopy of Nanoscale Hybrid Materials in Fluids of Varying Physical and Chemical Properties. *J. Phys. Chem. B* 2021, 125, 9223.

(60) Berry, G. C.; Fox, T. G. The Viscosity of Polymers and Their Concentrated Solutions. *Fortschritte der Hochpolymeren-Forschung*, Advances in Polymer Science; Springer-Verlag: Berlin, 1968; Vol. 5/3, p 261.

(61) Wang, J.-s.; Porter, R. S. On the Viscosity-Temperature Behavior of Polymer Melts. *Rheol. Acta* 1995, 34 (5), 496–503.

(62) Haque, M. A.; Feric, T. G.; Hamilton, S. T.; Park, A.-H. A.; Dadmun, M. D. Structure and Dispersion of Free and Grafted Polymer in Nanoparticle Organic Hybrid Materials-Based Solutions by Small-Angle Neutron Scattering. *J. Phys. Chem. C* 2021, 125 (9), 5327–5334.

(63) Paul, C.; Hiemenz, T. P. L. *Polymer Chemistry*; CRC Press, 2007.

(64) McDonald, S.; Wood, J. A.; FitzGerald, P. A.; Craig, V. S. J.; Warr, G. G.; Atkin, R. Interfacial and Bulk Nanostructure of Liquid Polymer Nanocomposites. *Langmuir* 2015, 31 (12), 3763–3770.

(65) Dukes, D.; Li, Y.; Lewis, S.; Benicewicz, B.; Schadler, L.; Kumar, S. K. Conformational Transitions of Spherical Polymer Brushes: Synthesis, Characterization, and Theory. *Macromolecules* 2010, 43 (3), 1564–1570.

(66) Rodriguez, R.; Herrera, R.; Archer, L. A.; Giannelis, E. P. Nanoscale Ionic Materials. *Adv. Mater.* 2008, 20 (22), 4353–4358.

(67) Simpson, J. *Organic Structure Determination Using 2D NMR Spectroscopy - A Problem-Based Approach*, 2nd ed., Elsevier, 2012.

(68) Butts, C. P.; Jones, C. R.; Harvey, J. N. High Precision NOEs as a Probe for Low Level Conformers—a Second Conformation of Strychnine. *Chem. Commun.* 2011, 47 (4), 1193–1195.

(69) Meot-Ner, M. The Ionic Hydrogen Bond. *Chem. Rev.* 2005, 105 (1), 213–284.

(70) Harned, H. S.; Hildreth, C. L. The Differential Diffusion Coefficients of Lithium and Sodium Chlorides in Dilute Aqueous Solution at 25°C. *J. Am. Chem. Soc.* 1951, 73 (2), 650–652.

(71) Ding, Y.; Zhang, C.; Zhang, L.; Zhou, Y.; Yu, G. Molecular Engineering of Organic Electroactive Materials for Redox Flow Batteries. *Chem. Soc. Rev.* 2018, 47 (1), 69–103.